



Comparative Analysis of Flow in U-Turn Rectangular Ducts with Direct Numerical Simulation

Muhammad Farras Arira¹, Ahmad Rajani^{2,3,4}, Randy Erfa Saputra⁵, Ariyawan Sunardi⁶, Syhrahman Akhdiyatullah Ginting¹, Dalmasius Ganjar Subagio², Ridwan Arief Subekti^{2,7}, Arifin Santosa², Kusnadi^{2,8}, Ahmad Fudholi^{2,9,*}

¹ Faculty of Mechanical and Aerospace Engineering, Institut Teknologi Bandung, Kota Bandung, Jawa Barat 40132, Indonesia

² Research Centre for Energy Conversion and Conservation, Badan Riset dan Inovasi Nasional, Kota Bandung, Jawa Barat 40173, Indonesia

³ Centre of Electrical Energy System (CEES), Institute of Future Energy, Universiti Teknologi Malaysia, Skudai, 81310 Johor Bahru, Johor, Malaysia

⁴ School of Electrical Engineering, Universiti Teknologi Malaysia, Skudai, 81310 Johor Bahru, Johor, Malaysia

⁵ School of Electrical Engineering, Telkom University, Bandung, Jawa Barat 40257, Indonesia

⁶ Electrical Engineering Department, Pamulang University, Kota Tangerang Selatan, Banten 15417, Indonesia

⁷ Department of Thermofluids, Faculty of Mechanical Engineering, Universiti Teknologi Malaysia, Skudai, 81310 Johor Bahru, Johor, Malaysia

⁸ High-Speed Reacting Flow Laboratory, School of Mechanical Engineering, Universiti Teknologi Malaysia, Skudai, 81310 Johor Bahru, Johor, Malaysia

⁹ Solar Energy Research Institute, Universiti Kebangsaan Malaysia, 43600 Bangi, Selangor, Malaysia

ARTICLE INFO

Article history:

Received 10 October 2024

Received in revised form 15 November 2024

Accepted 12 December 2024

Available online 31 January 2025

Keywords:

U-turn rectangular ducts; CFD; DNS; LBM; Reynolds number

ABSTRACT

Fluid flow within U-turn rectangular ducts plays a significant role in engineering applications, particularly in heat exchangers. Efficient design and optimization of these ducts are crucial for achieving optimal performance, especially concerning heat transfer. Previous research has predominantly utilized experimental methods to study flow behaviour in U-turn ducts, focusing on factors such as pressure loss and heat transfer. Computational fluid dynamics (CFD) has also been employed to explore flow characteristics, revealing the influence of parameters such as Reynolds number and gap size on flow behaviour. However, a detailed investigation into the flow structure within U-turn ducts has been lacking. To address this gap, this study employs Direct Numerical Simulation (DNS) to conduct a thorough investigation of flow in U-turn rectangular ducts. The study is conducted by varying the Reynolds numbers from 100 to 2000 and the gap size from 50% to 150% of the duct inlet diameter. Based on the simulation, it is found three distinct flow modes: Mode 1, representing attached laminar flow; Mode 2, representing detached laminar flow; and Mode 3, representing attached vortices flow. Of the three models, it is known that high Re numbers and narrow gaps have good heat transfer performance. These findings offer crucial guidance for designing efficient U-turn duct systems and lay the foundation for future research exploring more complex flow scenarios.

* Corresponding author.

E-mail address: ahmad.fudholi@brin.go.id (Ahmad Fudholi)

<https://doi.org/10.37934/cfdl.17.7.4760>

1. Introduction

Fluid flow within U-turn rectangular ducts finds diverse applications in engineering, with heat exchangers [1-3] being a prominent example. Research on U-turns has been conducted within the realm of magnetohydrodynamic (MHD) flow studies [4,5]. Yang *et al.*, [6] optimized the geometric model's structure using the CFX, respectively, to study U-shaped ducts under a uniform magnetic field with various wall conductance ratios. Efficient design and optimization of these ducts are imperative for achieving optimal performance. In various literature [7], the inner ducts are commonly configured as U-turn channels to enhance cooling. The magnitude of the gap in the U-turn duct section emerges as a critical factor influencing flow behaviour and performance.

Several research related to U-turn rectangular ducts have been conducted for the last decades. Initially researchers used an experimental method to study the flow in the U-turn rectangular ducts. Metzger *et al.*, [8] study pressure loss across the sharp U-turns in smooth rectangular channels experimentally by varying the geometry size of the U-turn duct and the Reynolds number of the flow, where the Reynolds number was varied around 5000-80000. In this study, it is found that there is an effect of gap size and Reynolds number on the pressure loss across the U-turn duct. The gap size refers to the distance between the duct walls at the U-turn. Two years later, Metzger *et al.*, [9] continued his study on sharp U-turn in smooth rectangular channels experimentally, but with focus on the heat transfer. It is found that as the gap size is reduced, local Nusselt number in the corner increased, particularly on the downstream sidewall. In 2006, Nakayama *et al.*, [10] conducted an experiment of flow withing sharp connected two-pass channels with $Re=35000$ and they discovered that the acceleration of the flow at the U-turn section becomes larger as the U-turn's gap is decreased. Besides that, as the gap size is decreased, the height of the separation bubble becomes larger and the reattachment point on the diver wall moves downstream.

Moreover, as computation performance became more powerful, analysis and exploration of flow in U-turn rectangular ducts were carried out using computational fluid dynamics (CFD) with a Reynolds Average Navier Stokes (RANS) approach [11-13]. CFD has also been used to analyse thermal transients [14] and Rosli *et al.*, [15] used it to analyse the relationship between the speed of the working fluid in a photovoltaic thermal (PVT) system and the resulting efficiency. The most recent research on the flow with a U-turn duct using CFD was conducted by Kim *et al.*, [16], with Reynolds numbers varying in the range of 14000 up to 78000. In this study, it is discovered that the influence of the gap size results in high pressure loss across the U-turn duct and this influence increases with an increasing Reynolds number.

Based on the published research that has been explained, it can be concluded that the Reynolds number and the size of the gap in the U-turn duct section emerges as a critical factor influencing flow behaviour and performance. However, to the best of our knowledge, the study of detailed flow structure on U-turn duct has not been conducted. Hence, the purpose of this study is to close this research gap by employing Direct Numerical Simulation (DNS) to perform a thorough investigation of flow in U-turn rectangular ducts. To attempt to shed light on the fundamental physics of flow in U-turn rectangular ducts, this study will compare various gap sizes and Reynolds numbers to gain important insights into the complex interplay between the two. These understandings are essential for design optimization and can help researchers and engineers decide on the appropriate duct design parameters for real-world applications.

2. Methodology

2.1 Lattice Boltzmann Method

In this study, we focus on two-dimensional (2D) direct numerical simulation of incompressible flow within U-turn duct based on the lattice Boltzmann method. In the last decades, the Lattice Boltzmann methods (LBM) has been proposed to be an alternative to conventional CFD method [17]. Originally introduced by Hardy *et al.*, [18] as a simplified lattice gas model, the method has evolved over the years and gained popularity due to its inherent simplicity, efficiency and ability to handle complex fluid dynamics [19-21]. Compared to conventional CFD methods, LBM typically requires less computational time and is more adaptable to complex geometries and boundary conditions. However, due to higher numbers of variables used, the LBM needs higher computer's memory compared to conventional CFD. Consequently, LBM is typically restricted to low to moderate Reynolds number cases where the numerical grid is not overly refined.

The LBM is based on the kinetic theory of gases, where the fluid is represented as a collection of fictitious particles on a discrete lattice. These particles follow probabilistic rules governed by a set of discrete Boltzmann equations, which describe the evolution of the particle populations over time. By solving these equations iteratively, the evolution of macroscopic properties of the fluid, such as density and velocity, can be obtained [17]. The particle distribution density can be represented in both three-dimensional physical space and in three-dimensional velocity space as a particle distribution function $f(x, \xi, t)$. The function represents the density of particles with velocity $\xi = (\xi_x, \xi_y, \xi_z)$ at position x and time t . The macroscopic mass density can be found by integrating over velocity space,

$$\rho(x, t) = \int f(x, \xi, t) d^3\xi \quad (1)$$

The total derivative of particle distribution function is,

$$\Omega(f) = \frac{df}{dt} = \frac{\partial f}{\partial t} + \xi_i \frac{\partial f}{\partial x_i} + \frac{F_i}{\rho} \frac{\partial f}{\partial \xi_i} \quad (2)$$

and it is called as the collision operator. Bhatnagar *et al.*, [22] proposed simpler collision operator called BGK operator.

$$\Omega^{BGK} = \frac{1}{\tau} (f^{eq} - f) \quad (3)$$

Maxwell argued that a gas in thermal equilibrium, the distribution function should not be function of time when the gas is distributed uniformly in the container. Thus, the equilibrium distribution can be found to be:

$$f^{eq}(x, \xi, t) = \rho \left(\frac{m}{2\pi k_B T} \right)^{\frac{3}{2}} \exp \left\{ -\frac{m(\xi-u)^2}{2k_B T} \right\} \quad (4)$$

where $f^{eq}(x, \xi, t)$ is isotropic in velocity space around $\xi = u$.

LBM discretised the continuous velocity space into a finite number of velocity sets, $C = \{c_1, c_2, \dots, c_Q\}$, where Q is the total number of discrete velocities. The discrete-velocity distribution

$f_i(x, t)$ represents the density of particles with velocity $c_i = (c_{ix}, c_{iy}, c_{iz})$ at position x and time t . The mass density can be written as:

$$\rho(x, t) = \sum_i f_i(x, t) \quad (5)$$

and the momentum density:

$$\rho u(x, t) = \sum_i c_i f_i(x, t) \quad (6)$$

The discretised Boltzmann equation with the BGK collision for each population can be written as:

$$\partial_t f_i(x, t) + c_i \nabla f_i(x, t) = \Omega_i^{BGK} \quad (7)$$

By also discretising the Boltzmann equation in physical space over the time step δt ,

$$f_i(x + c_i \delta t, t + \delta t) - f_i(x, t) = \int_t^{t+\delta t} \Omega_i^{BGK}(x(t'), t') dt' \quad (8)$$

where the right-hand side can be written as $\frac{\delta t}{2} (\Omega_i^{BGK}(x, t) + \Omega_i^{BGK}(x + c_i \delta t, t + \delta t))$, therefore:

$$f_i(x + c_i \delta t, t + \delta t) - f_i(x, t) = \omega (f_i^{eq} - f_i), \quad (9)$$

where $\omega = \frac{\delta t}{\tau + \frac{\delta t}{2}}$.

The LBM can be summarized into two parts, collision (or relaxation) and streaming (or propagation). The collision process can be written as:

$$f_i^*(x, t) = f_i(x, t) - \frac{\delta t}{\tau} (f_i(x, t) - f_i^{eq}(x, t)) \quad (10)$$

and the streaming process can be written as:

$$f_i(x + c_i \delta t, t + \delta t) = f_i^*(x, t) \quad (11)$$

where $f_i^*(x, t)$ is the distribution function after collision.

For boundary condition at a wall, LBM can utilize the Bounce-Back Method. The basic idea of Bounce-Back Method is to reflect the fluid distribution back into the domain at the solid boundary. Mathematically, the Bounce-Back Method is written as follows.

$$f_i(x, t + \delta t) = f_k(x, t) \quad (12)$$

Where k is defined as $c_k = -c_i$.

2.2 Simulation Setup

The simulation setup is depicted in Figure 1. The inlet flow is laminar with uniform velocity U_{inlet} . The inlet channel depth is d_{inlet} and the gap channel depth is denoted d_{gap} . The Reynolds Number Re of the duct can be formulated as follows:

$$Re = \frac{U_{inlet}d_{inlet}}{\nu} \quad (13)$$

Where ν denotes the kinematic viscosity. The simulations done in this paper assumed the temperature is at 25 degrees Celsius and pressure is 1 Atm. Besides that, the distribution of inlet velocity U_{inlet} is set to be uniform.

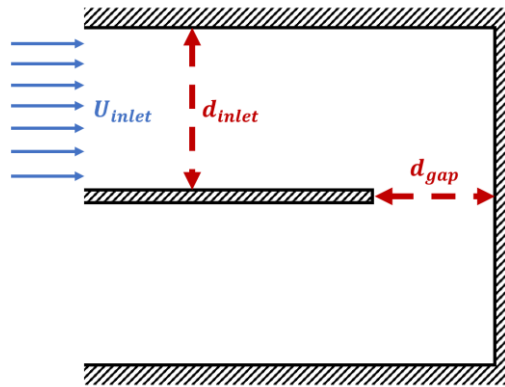


Fig. 1. Simulation setup

During the analysis, the value of d_{inlet} is held constant, while the values of Re and d_{gap} are systematically varied, as outlined in Table 1. The parameter d_{gap} is expressed as a percentage of d_{inlet} and is denoted by $\%_{gap}$. The Reynolds number is varied across a range of values: 100, 500, 1000 and 2000, while Alzahrani *et al.*, [23] employed variations of Re 3000 to 8000 to analyses heat transmission. The gap percentage is further adjusted at levels of 50%, 100% and 150%. It is important to note that in this analysis, the flow profiles are captured at the point where the flow reaches full development.

Table 1

Parameter variations in the analysis

	Case 1	Case 2	Case 3	Case 4	Case 5	Case 6	Case 7	Case 8	Case 9	Case 10	Case 11	Case 12
Re	100	100	100	500	500	500	1000	1000	1000	2000	2000	2000
% gap	150%	100%	50%	150%	100%	50%	150%	100%	50%	150%	100%	50%

3. Results

The analysis delves into the intricate details of fluid flow behaviour as it navigates through these ducts, taking into account the geometry and gap dimensions. By examining the flow velocity magnitude, the aim to provide a comprehensive understanding of how these parameters impact the flow patterns and characteristics within the U-turn rectangular ducts.

3.1 Direct Numerical Simulation (DNS) Results

In present section, we discuss the DNS results with varied Reynold number and gap size. In the discussion we focus more on the flow pattern and velocity profile in gap section. The velocity profile is represented by normalized velocity, which defined as u/u_{ref} , where u is our actual velocity and u_{ref} is the reference velocity, in this case the reference velocity is set to inlet velocity.

3.1.1 Reynolds number (Re) 100

The results of DNS with Re 100 are shown by Figure 2 below. These figures provide a visual representation of the flow velocity magnitude within the U-turn rectangular ducts for different gap sizes. It can be seen that for all gap percentages, the flow on the lower duct is attached to the wall. Besides that, all of flow on the lower duct is laminar, meaning there is no vortex built.

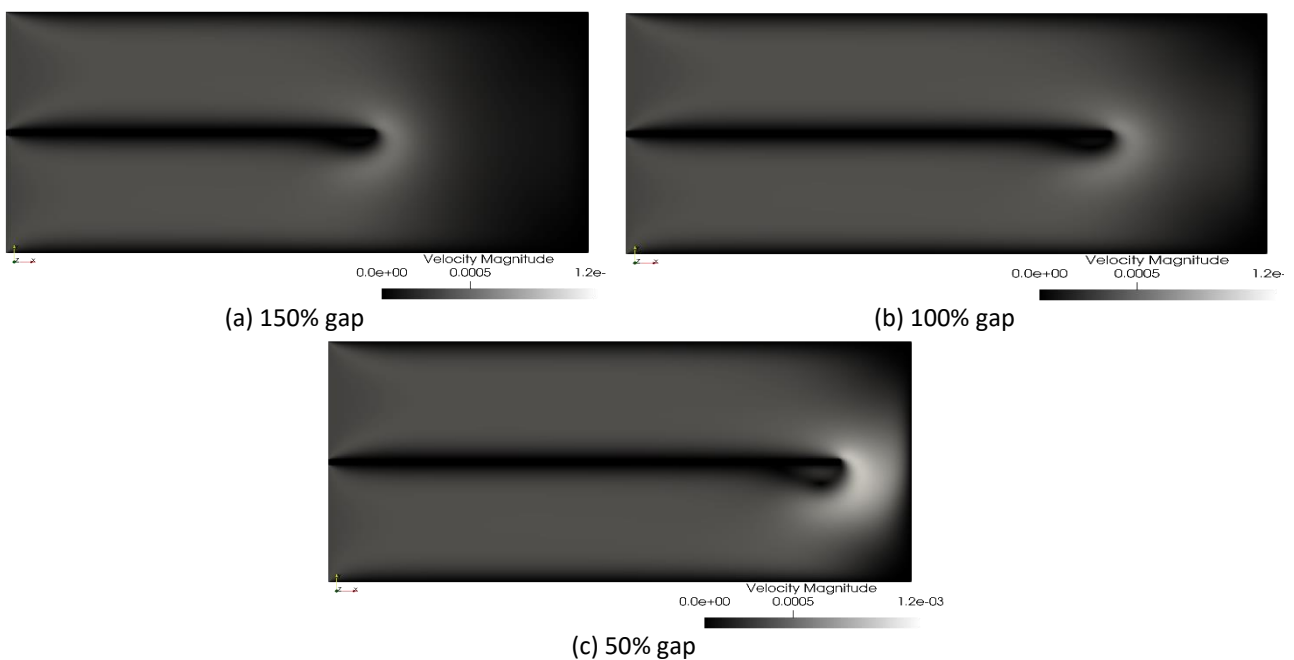


Fig. 2. Results of DNS with Re 100 with various gap (a) 150% (b) 100% (c) 50%

The Reynolds number, which represents the ratio of inertial forces to viscous forces, is a crucial parameter in determining the flow regime. At Reynolds numbers below a critical threshold, the flow tends to be laminar, characterized by smooth and predictable fluid motion. In our analysis, irrespective of the gap size, the Reynolds number of 100 resulted in laminar flow patterns, highlighting the dominance of viscous forces over inertial forces.

The velocity profile in the gap for Re 100 case is shown by Figure 3. The maximum velocity is increased as the gap size is decreased. Besides that, it can be seen also for all gap size cases, the maximum velocity is always greater than the inlet velocity, representing by the maximum normalized velocity value is always greater than one. It means that the flow is accelerated at the U-turn section for all gap sizes.

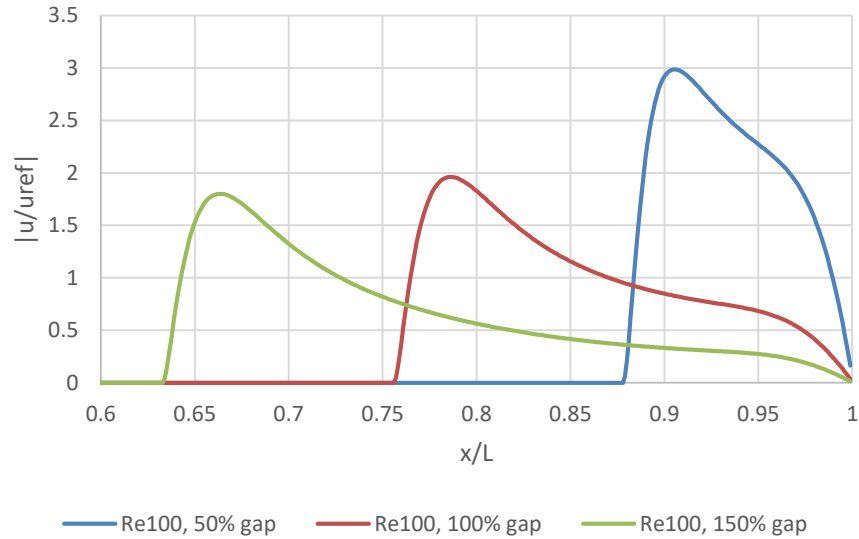


Fig. 3. Velocity profile for Re100 case

3.1.2 Reynolds number (Re) 500

The DNS study conducted at Reynolds number 500 for various gap sizes in U-turn rectangular ducts revealed a consistent flow behaviour where the flow on the lower duct was detached from the wall, as shown in Figure 4. This detachment of flow was observed across all gap sizes investigated.

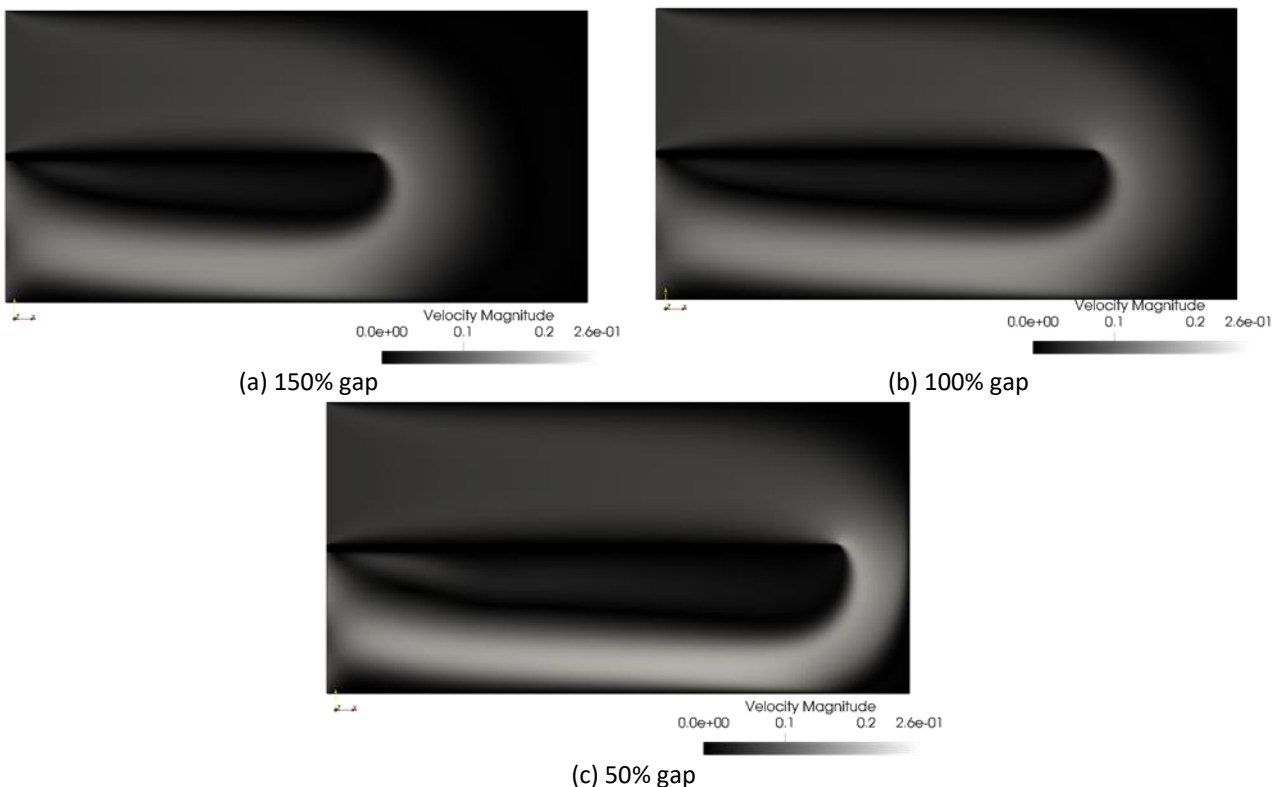


Fig. 4. Results of DNS with Re 500 with various gap (a) 150% (b) 100% (c) 50%

When flow detaches from the wall, it can result in increased pressure losses, reduced heat transfer efficiency and a decrease in the overall performance of the duct system. The formation of a

recirculation zone near the wall introduces regions of low-velocity fluid, limiting the effective transfer of heat or mass through the duct.

The velocity profile on the gap section for the Re 500 case is shown in Figure 5. From this velocity profile, we can know that for 150% and 100% gap size, the maximum velocity is constant, which is 2.5 times inlet velocity. Besides that, for 150% and 100% gap size, the velocity profile in the section is similar. On the other hand, the velocity profile for 50% gap size is with the others. The maximum velocity is increased for the 50% gap size.

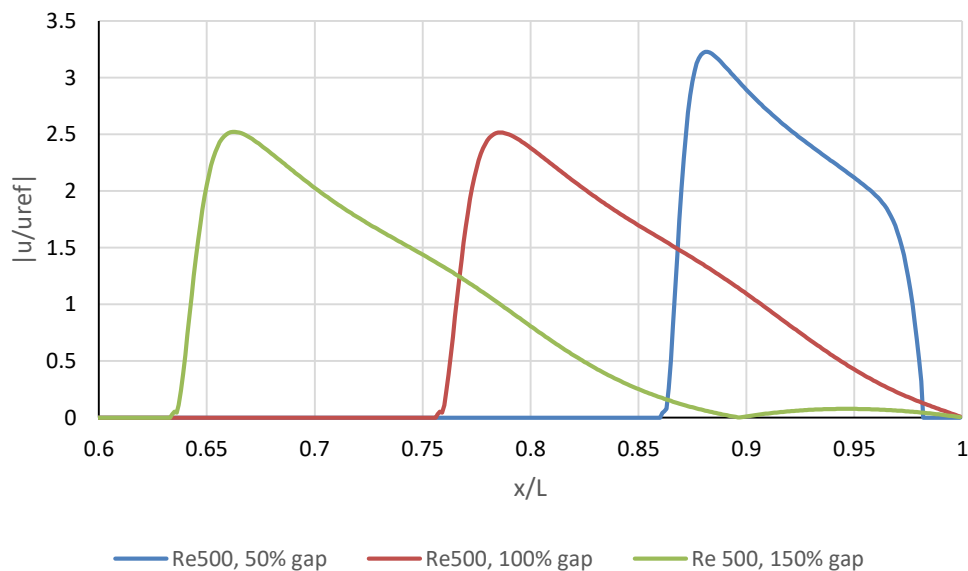


Fig. 5. Velocity profile for Re500 case

3.1.3 Reynolds number (*Re*) 1000

The results of the DNS conducted at Reynolds number 1000 are presented in Figure 6. These figures provide a visual representation of the flow behaviour within the U-turn rectangular ducts for different gap sizes. In Figure 6(a), for a high gap size, it can be observed that the flow on the lower duct is detached from the wall. This indicates a separation of the flow from the duct surface, leading to the formation of a recirculation zone. The detached flow results in a region of low-velocity fluid near the wall reduces the heat exchanger performance in this area due to the heat exchanger via convection mode does not occur.

In contrast, Figure 6(b) illustrates the flow behaviour for a small gap size. In this case, the flow on the lower duct is observed to be attached to the wall, maintaining direct contact with the duct surface. Additionally, vortices are observed in the flow field at small gap sizes, indicating the presence of swirling motions and increased fluid mixing. These vortices contribute to enhanced heat and mass transfer within the duct, potentially leading to improved performance in terms of heat exchange or fluid mixing applications.

The velocity profile for Re 1000 is shown in Figure 7. Since for the 150% and 100% gap size, the velocity pattern is as same as Re 500, which is detached laminar flow, we can see the same velocity profile as before: the maximum velocity is always 2.5 times inlet velocity.

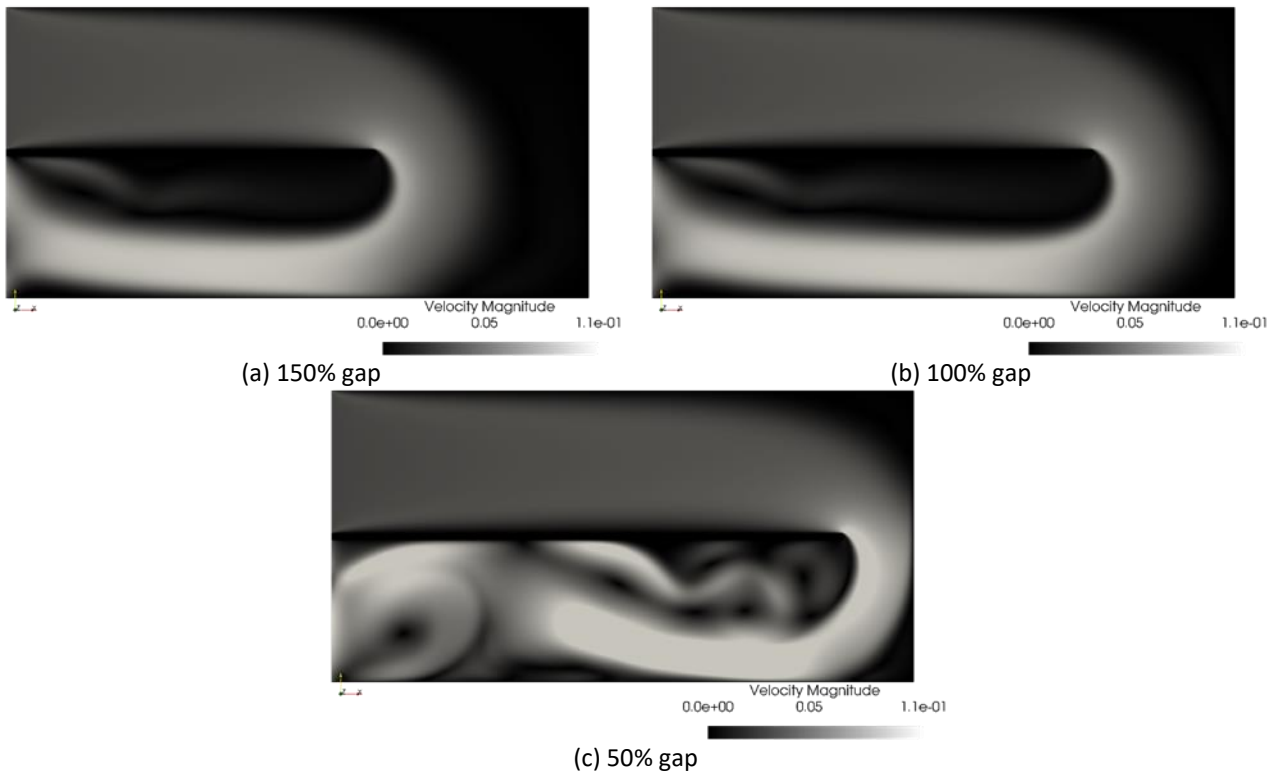


Fig. 6. Results of DNS with Re 1000 with various gap (a) 150% (b) 100% (c) 50%

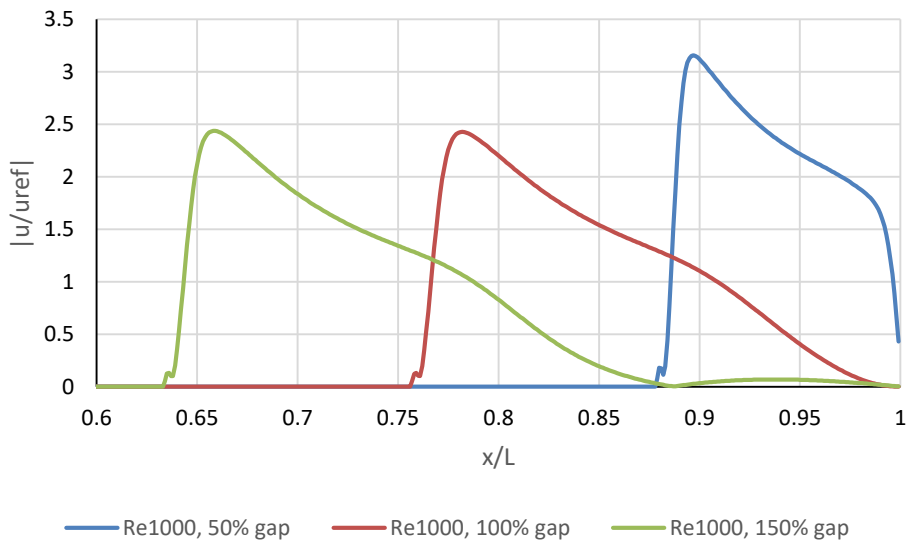


Fig. 7. Velocity profile for Re1000 case

3.1.4 Reynolds number (Re) 2000

At Reynolds number 2000, regardless of the gap size considered in this study, the flow on the lower duct was observed to generate vortices while remaining attached to the wall. The DNS result of the Re 2000 is shown in Figure 8. It is found that at higher Reynolds numbers, the flow tends to exhibit more complex behaviour, with the formation of vortices and increased fluid mixing.

In the case of U-turn rectangular ducts at Reynolds number 2000, the flow on the lower duct exhibited the formation of vortices, indicating the presence of swirling motions and enhanced fluid

mixing. These vortices contribute to increased heat and mass transfer within the duct, which can be advantageous for applications such as heat exchange and fluid mixing.

Additionally, the flow was observed to remain attached to the wall for all gap sizes. This implies that the flow maintains direct contact with the duct surface throughout the U-turn section, reducing the risk of flow separation and associated performance losses. The attachment of flow to the wall is particularly desirable in terms of minimizing pressure drop and maximizing the overall efficiency of U-turn duct systems.

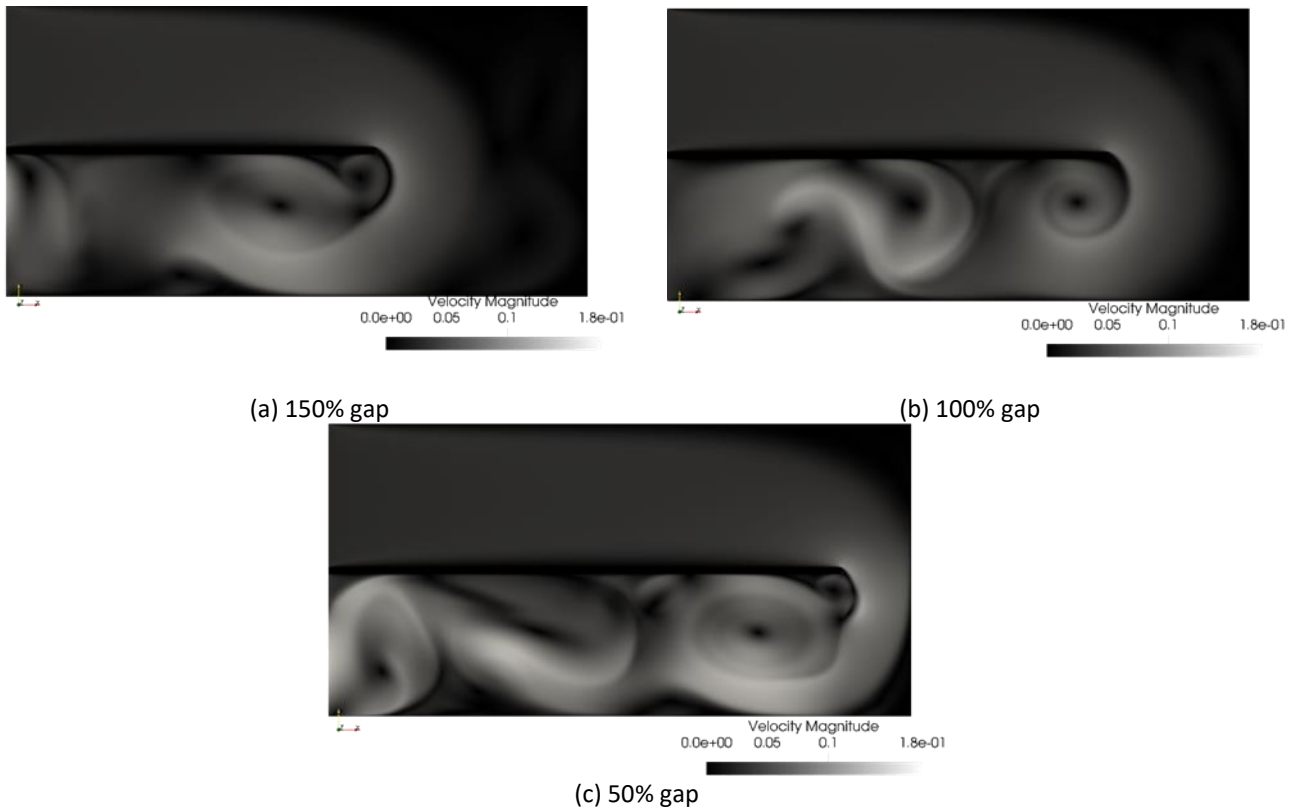


Fig. 8. Results of DNS with Re 2000 with various gap (a) 150% (b) 100% (c) 50%

3.2 Flow Modes

Based on the simulation results discussed previously, the flow behaviour within U-turn rectangular ducts can be categorized into three distinct modes: Mode 1, Mode 2 and Mode 3. These modes represent different flow characteristics observed at various combinations of Reynolds number and gap size.

Mode 1 corresponds to the attached laminar flow, where the flow remains attached to the wall and exhibits laminar characteristics. This mode is typically observed at low Reynolds numbers and large gap sizes. Figure 9(a) provides a visual representation of Mode 1, illustrating the attached laminar flow within the U-turn duct.

Mode 2 represents the detached laminar flow, where the flow detaches from the wall, leading to the formation of a recirculation zone. This mode is often observed at moderate Reynolds numbers and small gap sizes. The detached flow in Mode 2 is illustrated in Figure 9(b), highlighting the presence of a recirculation zone within the U-turn duct.

Mode 3 corresponds to the attached vortices flow, characterized by the formation of vortices while maintaining attachment to the wall. This mode is observed at moderate Reynolds numbers and gap sizes. Figure 9(c) visually depicts the attached vortices flow within the U-turn duct.

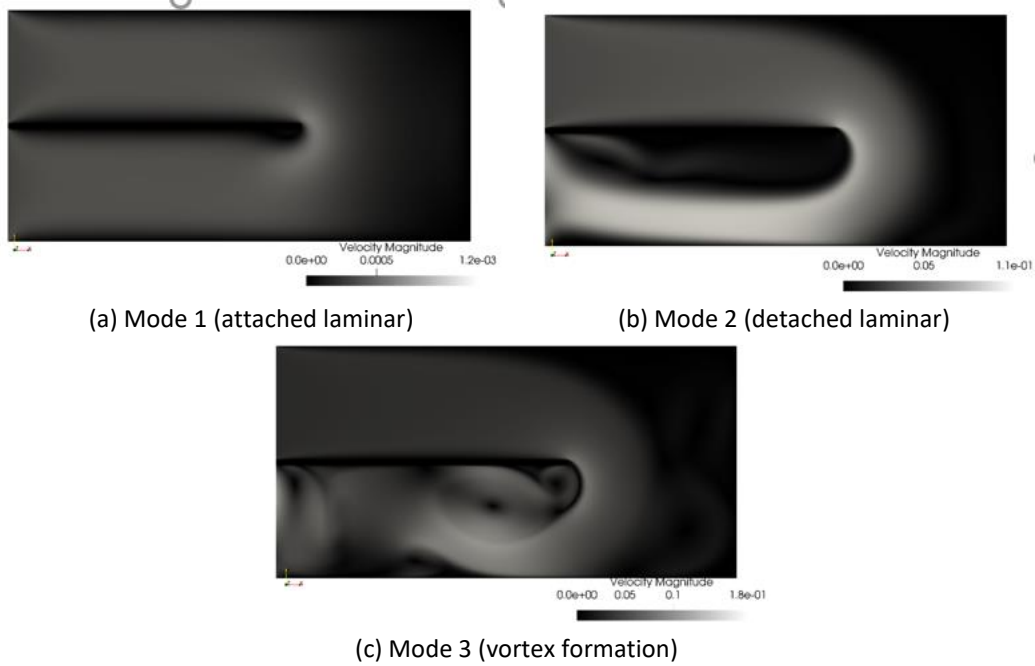


Fig. 9. Three Flow pattern occur in u-turn rectangular duct

Figure 10 shows the flow pattern regimes for different Reynolds numbers and gap size. For low Reynolds numbers, in this case Re_{100} , the flow pattern is always attached laminar flow, regardless of the gap size. For high Reynolds numbers, in this case Re_{2000} , the flow pattern is always attached vortices, regardless of the gap size. For moderate Reynolds number, such as in this case Re_{500} and Re_{1000} , the flow pattern usually occurs in detached laminar flow and vortex formation depending on the gap size. For moderate Reynolds number and large gap size, the flow is detached laminar flow. As the Re number increases and the gap size decreases the flow tends to become vortex formation.

Based on this finding of the wake flow pattern withing the U-turn duct, for heat exchanger applications, the suitable wake flow pattern is the attached vortices. The occurrence of vortices on the lower duct increases the local heat transfer, which could result in better outcomes for applications involving heat exchange. On the other hand, the wake flow pattern that should be avoided for heat exchangers applications is the detached laminar flow pattern. The separation flow phenomenon that occurs in this flow pattern reduces the heat transfer in the region of lower duct, specifically at low-velocity region.

To give an example of the engineering application of the findings in this research, they can be applied to the photovoltaic thermal system (PVT) application, especially the double-pass design. where the double-pass system has the same design as this research, where there are U-turn ducts and also have gaps [24,25]. From the previous paragraph, we can say that the attached vortices are appropriate for photovoltaic thermal system (PVT) applications because they can increase heat transfer. Good heat transfer can reduce the PV temperature. This is in accordance with the previous reference [26,27], reducing the PV temperature can increase the electrical efficiency of the system.

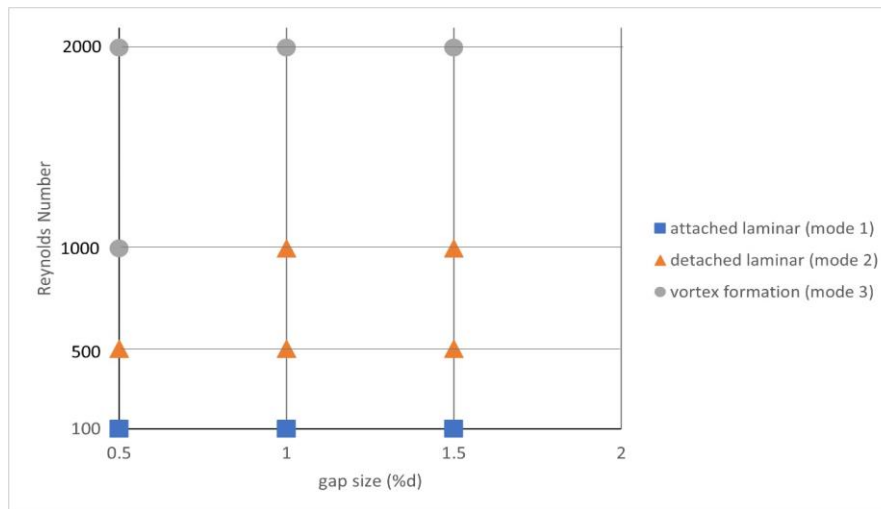


Fig. 10. Flow pattern regimes for different Reynolds number and gap size

4. Conclusions

The first-ever comprehensive numerical simulation of flow within U-turn rectangular ducts using the lattice Boltzmann method has been conducted. The results highlight three different flow models, starting with Reynolds numbers of 100, 500, 1000 and 2000. In addition to the Reynolds number, the gap size also varies, ranging from a gap size of 50% to 150% of the inlet diameter. From the three models, it is known that high Re numbers and narrow gaps have good heat transfer performance. For crucial insights into the flow physics within U-turn ducts, three distinct flow modes have also been identified: Mode 1, representing attached laminar flow; Mode 2, representing detached laminar flow; and Mode 3, representing attached vortices flow. Moreover, it is observed that the flow at the U-turn section accelerates with increasing Reynolds number and/or decreasing gap size. Based on the structure that occurs for each flow mode, the attached vortices flow (Mode 3) is the most convenient to use for heat exchangers applications. These findings serve as a reference for optimizing the design of various systems utilizing flow within U-turn ducts. Transition between these modes occurs at critical values of Reynolds number and gap size, which could be determined in future research. Additionally, while this study assumes a smooth wall, future investigations could analyse flow within ducts with ribs attached to the wall.

Acknowledgements

The authors would like to thank Badan Riset dan Inovasi Nasional (BRIN), Bandung, Indonesia, for facilitating all the data collection and providing sophisticated literature on the completion of this work. The gratitude is also devoted to all researchers (BRIN), staff and research assistants who helped in the accomplishment of this study. All authors contributed equally as the main contributors to this paper. All authors read and approved the final paper. This research was funded by a grant from Ministry of National Research and Innovation Agency Republic of Indonesia (BRIN) (Surat Keputusan No. 56/III.3/HK/2023).

References

- [1] Fudholi, Ahmad and Muslizainun Mustapha. "Mathematical modelling of bifacial photovoltaic-thermal (BPVT) collector with mirror reflector." *International Journal of Renewable Energy Research (IJRER)* 10, no. 2 (2020): 654-662.

- [2] Ma, Tao, Arash Kazemian, Ali Habibollahzade and Ali Salari. "A Comparative Study on Bifacial Photovoltaic/Thermal (Bpv/T) Modules with Various Cooling Methods." *Thermal (Bpv/T) Modules with Various Cooling Methods* (2021). <https://doi.org/10.2139/ssrn.3892712>
- [3] Mustapha, Muslizainun, Ahmad Fudholi, Nurul Syakirah Nazri, Muhammad Ibrahim Ali Zaini, Nurul Nazli Rosli, Wan Mustafa Wan Sulong and Kamaruzzaman Sopian. "Mathematical modeling and experimental validation of bifacial photovoltaic–thermal system with mirror reflector." *Case Studies in Thermal Engineering* 43 (2023): 102800. <https://doi.org/10.1016/j.csite.2023.102800>
- [4] Smolentsev, Sergey, Neil B. Morley, Clement Wong and Mohamed Abdou. "MHD and heat transfer considerations for the US DCLL blanket for DEMO and ITER TBM." *Fusion Engineering and Design* 83, no. 10-12 (2008): 1788-1791. <https://doi.org/10.1016/j.fusengdes.2008.04.002>
- [5] Smolentsev, Sergey, René Moreau, Leo Bühler and Chiara Mistrangelo. "MHD thermofluid issues of liquid-metal blankets: Phenomena and advances." *Fusion Engineering and Design* 85, no. 7-9 (2010): 1196-1205. <https://doi.org/10.1016/j.fusengdes.2010.02.038>
- [6] Yang, Shangjing and Chang Nyung Kim. "Magnetohydrodynamic flows in u-shaped ducts under a uniform transverse magnetic field." *Fusion Engineering and Design* 121 (2017): 87-99. <https://doi.org/10.1016/j.fusengdes.2017.06.007>
- [7] Li, Yang, Hongwu Deng, Guoqiang Xu and Shuqing Tian. "Heat transfer investigation in rotating smooth square U-duct with different wall-temperature ratios and channel orientations." *International Journal of Heat and Mass Transfer* 89 (2015): 10-23. <https://doi.org/10.1016/j.ijheatmasstransfer.2015.05.031>
- [8] Metzger, D. E., C. W. Plevich and C. S. Fan. "Pressure loss through sharp 180 deg turns in smooth rectangular channels." (1984): 677-681. <https://doi.org/10.1115/1.3239623>
- [9] Metzger, D. E. and M. K. Sahm. "Heat transfer around sharp 180-deg turns in smooth rectangular channels." (1986): 500-506. <https://doi.org/10.1115/1.3246961>
- [10] Nakayama, Hiroshi, Masafumi Hirota, Hideomi Fujita, Takeshi Yamada and Yusuke Koide. "Fluid flow and heat transfer in two-pass smooth rectangular channels with different turn clearances." (2006): 772-785. <https://doi.org/10.1115/1.2101854>
- [11] Wang, Ten-See and Mingking K. Chyu. "Heat convection in a 180-deg turning duct with different turn configurations." *Journal of Thermophysics and Heat Transfer* 8, no. 3 (1994): 595-601. <https://doi.org/10.2514/3.583>
- [12] Lin, Y-L., TI-P. Shih, M. A. Stephens and M. K. Chyu. "A numerical study of flow and heat transfer in a smooth and ribbed U-duct with and without rotation." *J. Heat Transfer* 123, no. 2 (2001): 219-232. <https://doi.org/10.1115/1.1345888>
- [13] Zhang, Xiao and Ramesh K. Agarwal. "Development of various rotation and curvature corrections for eddy-viscosity turbulence models." In *2018 AIAA Aerospace Sciences Meeting*, p. 0591. 2018. <https://doi.org/10.2514/6.2018-0591>
- [14] Nazer, Mohamed, Muhammad Fadzrul Hafidz Rostam, Se Yong Eh Noum, Mohammad Taghi Hajibeigy, Kamyar Shameli and Ali Tahaei. "Performance analysis of photovoltaic passive heat storage system with microencapsulated paraffin wax for thermoelectric generation." *Journal of Research in Nanoscience and Nanotechnology* 1, no. 1 (2021): 75-90. <https://doi.org/10.37934/jrnn.1.1.7590>
- [15] Rosli, Mohd Afzanizam Mohd, Cheong Jing Rou, Nortazi Sanusi, Siti Nur Dini Noordin Saleem, Nurfarhana Salimen, Safarudin Gazali Herawan, Norli Abdullah, Avita Ayu Permanasari, Zainal Arifin and Faridah Hussain. "Numerical investigation on using MWCNT/water nanofluids in photovoltaic thermal system (PVT)." *Journal of Advanced Research in Fluid Mechanics and Thermal Sciences* 99, no. 1 (2022): 35-57. <https://doi.org/10.37934/arfmts.99.1.3557>
- [16] Kim, Byunghui and Seokho Kim. "Numerical Investigation of Pressure Loss in a Rectangular Channel with a Sharp 180-Degree Turn: Influence of Design Variables and Geometric Shapes." *Energies* 16, no. 7 (2023): 3050. <https://doi.org/10.3390/en16073050>
- [17] Krüger, Timm, Halim Kusumaatmaja, Alexandr Kuzmin orest Shardt, Goncalo Silva and Erlend Magnus Viggen. "The lattice Boltzmann method." *Springer International Publishing* 10, no. 978-3 (2017): 4-15. https://doi.org/10.1007/978-3-319-44649-3_1
- [18] Hardy, J., Yves Pomeau and O. De Pazzis. "Time evolution of a two-dimensional classical lattice system." *Physical Review Letters* 31, no. 5 (1973): 276. <https://doi.org/10.1103/PhysRevLett.31.276>
- [19] Chen, Sheng, Zhaohui Liu, Zhiwei Tian, Baochang Shi and Chuguang Zheng. "A simple lattice Boltzmann scheme for combustion simulation." *Computers & Mathematics with Applications* 55, no. 7 (2008): 1424-1432. <https://doi.org/10.1016/j.camwa.2007.08.020>

- [20] Noël, Romain, Laurent Navarro and Guy Courbebaisse. "Lattice Boltzmann method for mathematical morphology: application to porous media." In *Multimodal Sensing and Artificial Intelligence: Technologies and Applications II*, vol. 11785, pp. 15-30. SPIE, 2021. <https://doi.org/10.1117/12.2593731>
- [21] Qiu, Liu-Chao. "A coupling model of DEM and LBM for fluid flow through porous media." *Procedia engineering* 102 (2015): 1520-1525. <https://doi.org/10.1016/j.proeng.2015.01.286>
- [22] Bhatnagar, Prabhu Lal, Eugene P. Gross and Max Krook. "A model for collision processes in gases. I. Small amplitude processes in charged and neutral one-component systems." *Physical review* 94, no. 3 (1954): 511. <https://doi.org/10.1103/PhysRev.94.511>
- [23] Alzahrani, Hassan AH, G. T. Danappa, MG Anantha Prasad, K. Rajesh, Salim Al Jadidi, N. Madhukeshwara and B. M. Prasanna. "Enhancing solar air heater efficiency with 3D cylinder shaped roughness elements." *Case Studies in Thermal Engineering* 51 (2023): 103617. <https://doi.org/10.1016/j.csite.2023.103617>
- [24] Yüksel, Coşkun, Murat Öztürk and Erdem Çiftçi. "Analysis of a novel V-grooved double pass photovoltaic thermal solar dryer including thermal energy storage." *Applied Thermal Engineering* 236 (2024): 121697. <https://doi.org/10.1016/j.applthermaleng.2023.121697>
- [25] Koşan, Meltem and Mustafa Aktaş. "Performance investigation of a double pass PVT assisted heat pump system with latent heat storage unit." *Applied Thermal Engineering* 199 (2021): 117524. <https://doi.org/10.1016/j.applthermaleng.2021.117524>
- [26] Mohammed, Majid Ahmed, Bashar Mahmood Ali, Khalil Farhan Yassin, Obed Majeed Ali and Omar Rafae Alomar. "Comparative study of different phase change materials on the thermal performance of photovoltaic cells in Iraq's climate conditions." *Energy Reports* 11 (2024): 18-27. <https://doi.org/10.1016/j.egy.2023.11.022>
- [27] Alktranee, Mohammed and Bencs Péter. "Energy and exergy analysis for photovoltaic modules cooled by evaporative cooling techniques." *Energy Reports* 9 (2023): 122-132. <https://doi.org/10.1016/j.egy.2022.11.177>